

ResORR: A Globally Scalable and Satellite Data-driven Algorithm for River Flow Regulation due to Reservoir Operations

Pritam Das¹, Faisal Hossain^{1*}, Sanchit Minocha¹, Sarath Suresh¹, George K. Darkwah¹, Hyongki Lee², Konstantinos Andreadis³, Miguel Laverde-Barajas⁴ and Perry Oddo⁵

¹Department of Civil and Environmental Engineering, University of Washington, Seattle, WA, USA

²Department of Civil and Environmental Engineering, University of Houston, Houston, TX, USA

³Department of Civil and Environmental Engineering, University of Massachusetts, Amherst, MA, USA

⁴Asian Disaster Preparedness Center, Bangkok, 10400, Thailand

⁵Science Systems and Applications, Inc., Lanham, MD, USA

* Corresponding Author.

Abstract

Storage and release of surface water by reservoirs can alter the natural streamflow pattern of rivers with negative impacts on the environment. Such reservoir-driven river regulation is poorly understood at a global scale due to a lack of publicly available in-situ data on reservoir operations. However, with rapid advancements in satellite remote sensing-based tracking of reservoir state, this gap in data availability can be bridged. In this study, we modeled regulated flow of rivers using only satellite-observed reservoir state and hydrological modeling forced also with satellite precipitation data. We propose a globally scalable algorithm, ResORR (Reservoir Operations driven River Regulation), to predict regulated river flow and tested it over the heavily regulated basin of the Cumberland River in the US. ResORR was found able to model regulated river flow due to upstream reservoir operations of the Cumberland River. Over a mountainous basin dominated by high rainfall, ResORR was effective in capturing extreme flooding modified by upstream hydropower dam operations. ResORR successfully captured the peak of the regulated river flow altered by hydropower dam and flood control operations during the devastating floods of 2018 in the South Indian state of Kerala. On average, ResORR improved regulation river flow simulation by more than 50% across all performance metrics when compared to a hydrologic model without a regulation module. ResORR is a timely algorithm for understanding human regulation of surface water as satellite-estimated reservoir state is expected to improve globally with the recently launched Surface Water and Ocean Topography (SWOT) mission.

Keywords

River Regulation, Reservoir Operations, Hydrological Modeling, Satellite Remote Sensing

Plain Language Summary: River flow that is regulated by upstream reservoir operations is difficult to model at a global scale without adequate parameterizations because of the lack of publicly available in-situ reservoir operation data. In this study, we developed a river flow regulation algorithm called ResORR that can be applied globally based entirely on satellite-based observation of reservoir states that are becoming now widely available. Tests over regulated river basins show that ResORR is able to improve the prediction of regulated river flow by at least

50% compared to the baseline of using a hydrologic model without a regulation or reservoir module.

1. Introduction

Rivers have provided humans with food, water and energy security since human civilization first started to take shape in ancient valleys of Tigris-Euphrates, Indus and Nile rivers. This has only been made possible by means of control structures such as dams and reservoirs, which allow storage and release of water from the river according to human needs. Usually, water from the river is stored in reservoirs when the river naturally has higher flows, resulting in a net reduction in the downstream flow of the river. This storage is driven by human needs such as flood control or to meet future freshwater demand when natural availability may be insufficient. The converse happens during naturally occurring periods of low flows, when release of water from reservoirs artificially increases the downstream flow rate during the dry season to meet demand for water. This regulation of surface water, in the form of alteration of the streamflow from its natural pattern of discharge under pristine conditions, can be termed as river regulation.

River regulation can change how the basin responds to a hydro-meteorological event in the form of precipitation or snowmelt, affecting its natural variability and streamflow timing. For instance, Wisser and Fekete (2009) found that the average residence time has increased by 42 days globally over the past century due to construction of reservoirs. Such disruption and alteration of natural conditions is even more profound at a regional scale, for instance, Bonnema and Hossain, (2017) note about 11-30% streamflow alteration in the Mekong basin, with the residence time of reservoirs varying from 0.09 to 4.04 years. Vu et al., (2021) estimate that reservoirs in the Mekong hold 50% of its dry season flow and 83% of its wet season flow. As a result, the high flows of the Mekong-river have reduced by 31%, while the low-flows have increased by 35%.

River regulation can also have serious ecological repercussions. For instance, the unique annual flow reversal of the Tonle Sap River (TSR) leading to filling up the Tonle Sap Lake (TSL) during the wet season and draining it during dry season may cease to exist if the flood pulse of the Mekong River dampens by 50% and is delayed by a month (Pokhrel et al., 2018). The absence of this unique flow reversal may have a negative impact on aquatic biodiversity, particularly for fisheries and paddy planting (Marcaida et al., 2021). Similarly, in European rivers, high-flows appear to be down by 10% while low-flows are up by 8% (Biemans et al., 2011). Negative consequences are not limited to only ecological aspects but can also influence the regional demand-and-supply of resources, with the potential to escalate pre-existing water conflicts. The construction and filling up of the Grand Ethiopian Renaissance Dam (GERD) on the Nile River has been a source of contention between Ethiopia and the other riparian countries – Egypt and Sudan. Eldardiry and Hossain, (2021) estimate that if unprepared, the High Aswan Dam (HAD) – a dam of existential importance to Egypt for its water-food-energy security – may take anywhere from 2 years to 7 years to fully recover following the filling-up of the GERD. Although, they also optimistically estimate that with cooperation and planning between the riparian countries, the recovery period can be limited to immediate 2 years.

Apart from the direct alteration of streamflow timing of rivers, regulation due to dam and reservoir operations can have an indirect effect on other components of the eco-system. For

instance, river regulation disturbs the natural sediment flow, resulting in a net reduction in sediment deposition along shorelines of rivers, estuaries and oceans (Dunn et al., 2019; Li et al., 2021). River water temperature anomalies owing to thermal stratification in reservoirs have also been widely recognized (Ahmad et al., 2021; Cheng et al., 2020). Considering the sensitivity of aquatic life to the water temperature changes (Caissie, 2006), river regulation can negatively affect the environmental suitability for aquatic organisms (Cheng et al., 2022). Such negative environmental consequences are a direct result of human decisions – which many consider necessary to support the demands of a rapidly growing population. A better understanding of human regulation of river flow, exacerbated by a changing climate and increasing freshwater demand, is urgently required to ensure a sustainable future.

The coupled nature of human-water resources has led to developments in explicitly modeling reservoir operations in Large-Scale Hydrological Models (LHMs) and Global Circulation Models (GCMs) (Hanasaki et al., 2018; Wada et al., 2017). Existing methods to represent human activities in hydrological models rely on modeling the optimal reservoir release based on operating parameters such as the design role of the reservoir (Hanasaki et al., 2006), land-water management schemes, downstream demand for water and energy (Alcamo et al., 2003; Biemans et al., 2011; Haddeland et al., 2006; Vanderkelen et al., 2022). Many of these human activities are often assumed or ‘parameterized’ due to lack of sufficient observational data on reservoir operations. Using such a parameterized approach, Zhou et al. (2016) found that in highly regulated basins, such as the Yellow and the Yangtze rivers, the seasonal reservoir storage variations can contribute up to 72% of the variability of the basin’s total storage. While such key insights can be obtained using generic schemes of reservoir operations, the underlying assumption of optimal reservoir operations may not always hold true. Stakeholders and reservoir managers must often deviate from optimal operating conditions based on a variety of reasons, such as adapting to regional water and energy demands, new hydro-political reality, environmental regulations, and changing weather and climate patterns that result in river flow to exceed the bounds of pre-dam historical flow records.

In the past, modeling human decisions of reservoir operations using parameterizations or criteria-based assumptions has been the primary way for characterizing river-regulation due to a lack of publicly available observations on dam operations. However, to better understand river regulation, which is representative of the intricacies of operation of individual reservoirs, we need to characterize and quantify river regulation grounded in observations of reservoir operations (Biswas et al., 2021; Das et al., 2022; Zhou et al., 2016). Earth observing satellites, with their vantage of space and a multi-decadal record of observations on reservoir operations now provide an opportunity to fill this data availability gap by inferring reservoir operations from space (Bonnema & Hossain, 2017). Rather than relying on parameterized or criteria-based assumptions of reservoir operations, we can now use actual observation-based reservoir operations to quantify the regulation of flow in physical models. Because satellite observations today can track the dynamic state of reservoirs comprising surface area, water surface elevation, evapotranspiration losses, storage change and even outflow (Cooley et al., 2021; Hossain et al., 2017; Lee et al., 2010; Okeowo et al., 2017; Zhao et al., 2022), there is now a stronger argument to move away from assumptions and parameterizations in representing human flow regulation in physical hydrologic models.

Satellites such as the Landsat, Sentinel, and Jason series have been extensively monitoring hydrologically relevant aspects of the Earth’s surface, such as surface reflectance and

elevation, at the global scale. For instance, Gao et al., (2012) were able to recreate storage variations of large reservoirs using observations from the Moderate Resolution Imaging Spectroradiometer (MODIS) satellite platform. Cooley et al., (2021) used NASA's ICESat-2 satellite observations of water level height to estimate that about 3/5th of the Earth's surface water storage variability takes place due to reservoirs. Moreover, the recently launched terrestrial hydrology-focused Surface Water and Ocean Topography (SWOT) satellite is now expected to improve the monitoring of surface water resources at an unprecedented scale and accuracy (Biancamaria et al., 2016). Together, these Earth-observing satellites provide an opportunity to independently track various aspects of the hydrological cycle, including reservoir operations (Bonnema & Hossain, 2017; Hossain et al., 2017).

Using such multi-sensor satellite data on surface water, we can now build comprehensive, distributed, and scalable modeling platforms to simulate reservoir-river systems. The Reservoir Assessment Tool (RAT) is one such modeling platform that can estimate reservoir fluxes, comprising inflow to the reservoir, storage change, evaporative losses and outflow, solely using satellite data and hydrological modeling (Biswas et al., 2021; Das et al., 2022). More recent developments have made it easier to monitor reservoirs using RAT, further democratizing the availability of surface water data at the granular level for regulated river systems (Minocha et al., 2023). This has allowed for both global and regional scale studies of the anthropogenic impact on terrestrial water storage (Biswas & Hossain, 2022) and floods (Suresh et al., 2023), especially in the regions of the world that lack a robust data collection and sharing infrastructure.

Considering the importance and urgency of an observations-driven understanding of river regulation, there is now a need to develop methods to quantify river regulation due to reservoir operations that can be scaled globally based on publicly and globally available satellite observables. The wide availability of satellite-based reservoir operations data will only keep increasing with the recent launch of the SWOT mission that is optimized for surface water tracking, particularly for lakes and reservoirs. Here, the multi-satellite observations used by RAT to estimate storage change (Das et al., 2022) can be directly used as observations to quantify river regulation, obviating the need to separately model reservoir operations based on parameterizations or operating assumptions, which can be both difficult and unrepresentative of actual reservoir operations. Given the availability of multi-decadal satellite observations of surface water that are now made widely accessible due to advancements in information technology, we are now uniquely positioned to predict regulated flow at a level of granularity that was not possible before. Estimation of river regulation grounded in observational data inherently represents the actual or likely decisions made by reservoir operators. The primary research question that this paper addresses is – *How can river regulation due to operation of reservoirs be formulated in a globally scalable format using primarily satellite observations?* The objectives of the paper are as follows –

1. To develop a globally scalable river-regulation algorithm based on satellite observables or satellite derived reservoir data for predicting the human regulation of surface water.
2. To investigate incorporation of the river-regulation algorithm in the RAT modeling platform for regulated rivers, and quantify its skill in capturing river flow regulation at a basin scale.

2. Study area and Data

2.1. The Cumberland River in Tennessee, US

The Cumberland River is highly regulated by a system of 10 major dams and reservoirs with varying primary use cases, making it one of the most heavily regulated basins. The United States Army Corps of Engineers (USACE) Nashville District, own and operate 10 such multi-purpose dam/reservoir projects on the Cumberland River, with the first dams being built in 1950s. These dams are used for hydropower generation, flood control, recreation, commercial navigation, public water supply, and fisheries and wildlife management – bringing in immense economic benefits to the region (Robinson, 2019). Figure 1 compares the daily discharge in the Cumberland River for two time-periods corresponding to unregulated conditions (1916-1920) and regulated conditions (2016-2020). The effect of regulation can be clearly seen in the figure, in the form of reduced range and variability in the discharge hydrograph. Studies suggest that such regulation has caused a sharp decline in the population and species variety of Mussels in the basin, which were plentiful when the river was unregulated (Neel & Allen, 1964; Tippit et al., 1995; Wilson & Clark, 1914). In addition to the highly regulated status of the basin, the availability of long periods of in-situ observational data from the operating agencies makes this basin an ideal test bed for investigating anthropogenic river regulation (Bonnet et al., 2015).

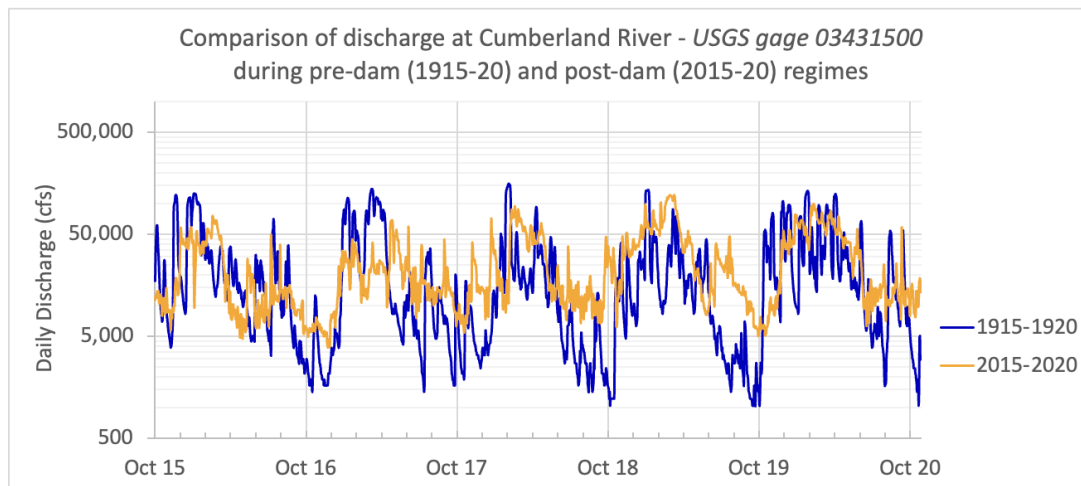


Figure 1: Comparison of 5 years of daily discharge during (a) unregulated conditions, prior to construction and operation of major dams (1916-1920), and (b) regulated conditions, as observed in the Cumberland River near Nashville, TN. The flow rate in a regulated regime has a markedly attenuated peak-trough range – with low flows rarely dropping below 5000 cfs as compared to the unregulated regime when flow rates naturally used to drop to 1000 cfs. Source: United States Geological Survey (USGS).

Originating in the Appalachian Mountains, the Cumberland River flows westwards through the states of Kentucky and Tennessee in the United States, draining a region of about 18,000 sq. miles (~45,000 sq. km), before merging into the Ohio River. Ten dams – Martins Fork, Laurel, Wolf Creek, Dale Hollow, Cordell Hull, Center Hill, Old Hickory, J. Percy Priest, Cheatham, and Barkley dams – are operated by USACE, with some additional dams operated by the Tennessee Valley Authority (TVA) (Robinson, 2019). Limited by the availability of in-situ reservoir operations data, 8 of the USACE owned dams were included in this study. Based on the

conclusions of the study, the authors believe that the results are not affected by the exclusion of the 2 USACE dams owing to their relatively insignificant (Martin’s Fork dam) to no storage (Cheatham dam). The region generally has a temperate, warm, and humid climate, with most of the precipitation occurring from December through May.

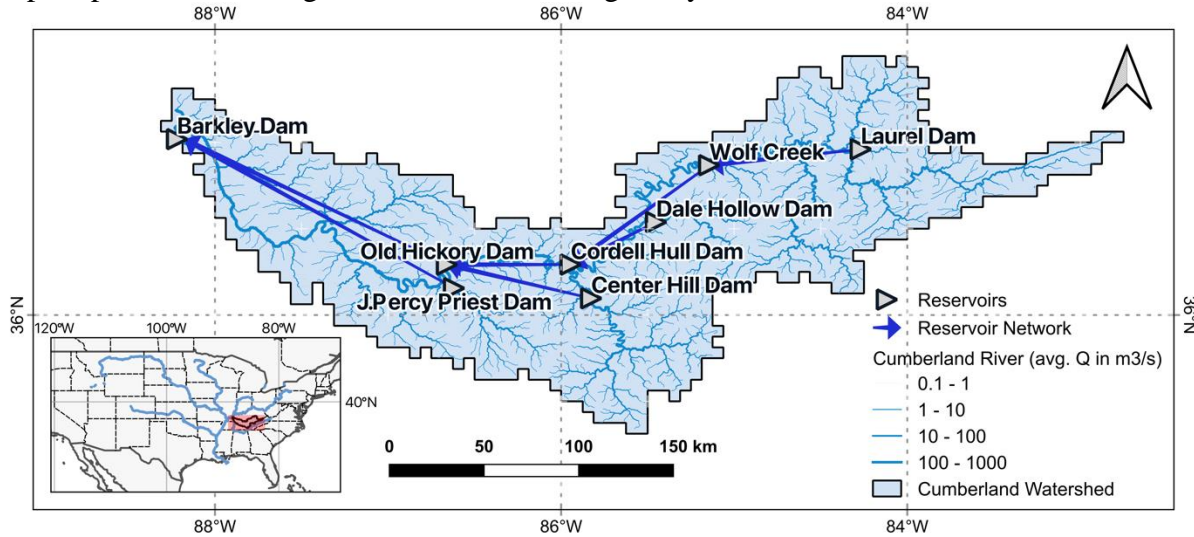


Figure 2: Map of the Cumberland basin, showing locations of the reservoirs, the reservoir network and the location of the Cumberland basin in the US.

2.2. In-situ and satellite observations of reservoir dynamics

To develop, test and validate the river-regulation algorithm, observed in-situ data pertaining to reservoir operations – inflow, outflow, and storage – were used, which were obtained from the ResOpsUS (Steyaert et al., 2022) dataset. This dataset is a compilation of in-situ reservoir operations data for 679 major dams in the US, including 8 of the USACE dams in the Cumberland basin and one dam operated by the TVA, until November 2019. Daily storage change was calculated using the storage values in the dataset for all but 2 dams – Old Hickory and J. Percy Priest – which had missing storage data from July 2015 onwards. The storage change for these reservoirs were obtained by subtracting the reported Outflow from the Inflow ($\Delta S = I - O$). Readers are referred to section 8.2 for more discussion on this data preparation step. The in-situ data was also used to force the river-regulation model in certain experiments to compare the sensitivity of the river-regulation model to the accuracy of input data – a detailed discussion is provided in section 4.1. Additionally, the in-situ Area-Elevation Curve (AEC) of all the USACE reservoirs were also obtained from the Access to Water Resources Data – Corps Water Management System (CWMS) Data Dissemination tool (USACE, n.d.).

The latest version of Reservoir Assessment Tool (RAT 3.0) was used to obtain the storage change and river flow under pristine (naturalized) conditions (assuming no upstream reservoirs). Originally developed by Biswas et al., (2021), the RAT framework is designed to improve access to information on reservoir dynamics, especially with recent developments leading to both a higher performance and accessibility (Das et al., 2022; Minocha et al., 2023). Using the default hydrological model of RAT, Variable Infiltration Capacity (VIC) (Liang et al., 1994), the inflow to each reservoir’s location was estimated. The default VIC parameters, and sources of temperature and wind data used in RAT 3.0 were used to force the hydrological

model. The precipitation was obtained from the ERA-5 reanalysis dataset (Hersbach et al., 2020). It must be noted here that the VIC-based reservoir inflow in RAT 3.0 does not take upstream reservoir operations into account, and hence the need to develop a model that can supplement the RAT framework by taking upstream regulation into consideration. A detailed discussion on how the hydrological model's estimated inflow in pristine conditions is used in the river regulation model can be found in section 3.1. Since the in-situ AEC of the TVA-owned reservoir was not available, the default AEC option in RAT 3.0 was applied based on the Shuttle Radar Topography Mission Digital Elevation Model (SRTM DEM) (Earth Resources Observation And Science (EROS) Center, 2017).

3. Methods

3.1. Reservoir Operations driven River Regulation (ResORR) – Conceptual algorithm

The core assumption of the ResORR algorithm is that the volume of water entering the reservoir, Inflow (I), is composed of two components – natural and regulated. The Natural Runoff (NR) is defined as the component of surface runoff that flows naturally into the reservoir without passing through any upstream reservoirs. Similarly, the Regulated Runoff (RR) is the component of surface runoff that first gets intercepted by an upstream reservoir before being released based on the reservoir's operations policy. The partitioning of the inflow to a reservoir is defined by the following equation,

$$I = NR + RR \quad (1)$$

Essentially, the problem of estimating the inflow at any reservoir is decomposed into the two parts of estimating the natural and regulated components of the incoming streamflow. A detailed discussion on estimating these sub-components of inflow is provided later in the section. The estimated inflow to a reservoir in this scheme will, hence, be affected by regulation due to upstream reservoir operations.

For example, consider the example of a two-reservoir system (A and B), where reservoir B is downstream of reservoir A, depicted in the schematic in Figure 3(a). In this scenario, the inflow at reservoir B would have contributions from the outflow of the upstream reservoir A in the form of RR (i.e., $RR \neq 0$), in addition to the NR . On the other hand, since reservoir A has no upstream reservoirs, the inflow to the reservoir would be fully natural, i.e., $RR = 0$ and $I = NR$.

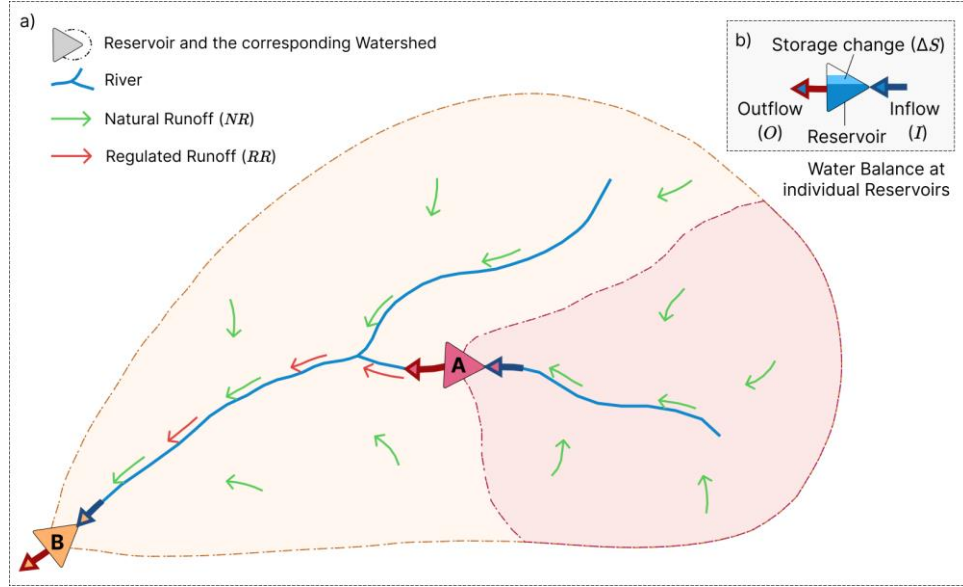


Figure 3: Conceptual schematic of the ResORR model. Panel (a) depicts the flow of surface runoff and streamflow, along with the contribution of the natural (green arrows) and regulated (red arrows along the stream) components, referred to in this paper as Natural Runoff (NR) and Regulated Runoff (RR) to the Inflow ($I = NR + RR$) to a reservoir. Panel (b) describes the components of the water balance equation ($O = I - \Delta S$) used at the reservoir to obtain the outflow from the reservoir, which is treated as the regulated component of the downstream streamflow.

As discussed above, the RR is defined as the component of inflow to a reservoir due to upstream reservoir releases. It is estimated as the sum of all Outflow (O) of the upstream reservoirs.

$$RR_i = \sum_j^N O_j \quad (2)$$

Where RR_i is the incoming Regulated Runoff to reservoir i ; O_j is the Outflow from the j^{th} upstream reservoir; N is the total number of upstream dams for reservoir i .

The NR is defined as the volume of water inflow to the reservoir due to surface runoff unaffected by any upstream reservoir operations., i.e., the generated surface runoff drains directly to the reservoir, without passing through any other reservoir. This surface runoff is generated in the part of the watershed which is not shared by any other upstream dams. For instance, in Figure 3, the orange and red shaded regions of the watershed will generate the NR for reservoirs B and A respectively. The NR for a reservoir can be estimated using the theoretical inflow into a reservoir if there were no upstream dams, which is referred to as the Theoretical Natural Runoff (TNR) in this paper. The Theoretical Natural Runoff (TNR) refers to the inflow to a reservoir if none of the upstream dams existed. The TNR can be calculated using the following equation –

$$TNR_i = NR_i + \sum_j^N NR_j \quad (3)$$

Where, TNR_i is the Theoretical Natural Runoff of reservoir i ; NR_i is the Natural Runoff to reservoir i ; and N is the total number of upstream dams of reservoir i along the same river network. For example, in the schematic in Figure 3, the TNR of reservoir A and B would be NR_A and $NR_B + NR_A$ respectively.

Since the TNR represents streamflow into a reservoir in pristine conditions (without considering upstream reservoirs), it is analogous to the modeled inflow at reservoirs using traditional hydrologic models which do not take reservoir operations into account. The NR of any reservoir can be obtained by rearranging the terms of (3, and calculating the NR for reservoirs by iteratively moving downstream for each time-step. The NR for any reservoir can hence be obtained using the TNR of the reservoir, and the NR of the upstream reservoirs using the following equation –

$$NR_i = TNR_i - \sum_j^N NR_j \quad (4)$$

Using the estimated NR and RR components, the inflow to a reservoir under regulated conditions is then calculated using (1. Using the storage change of the reservoir, obtained either in-situ or using satellite estimates, the outflow can then be calculated using the water balance equation –

$$O = I - \Delta \quad (5)$$

Where O , I and ΔS are the outflow, inflow and storage change of a reservoir respectively. These equations were solved for the reservoirs mapped in

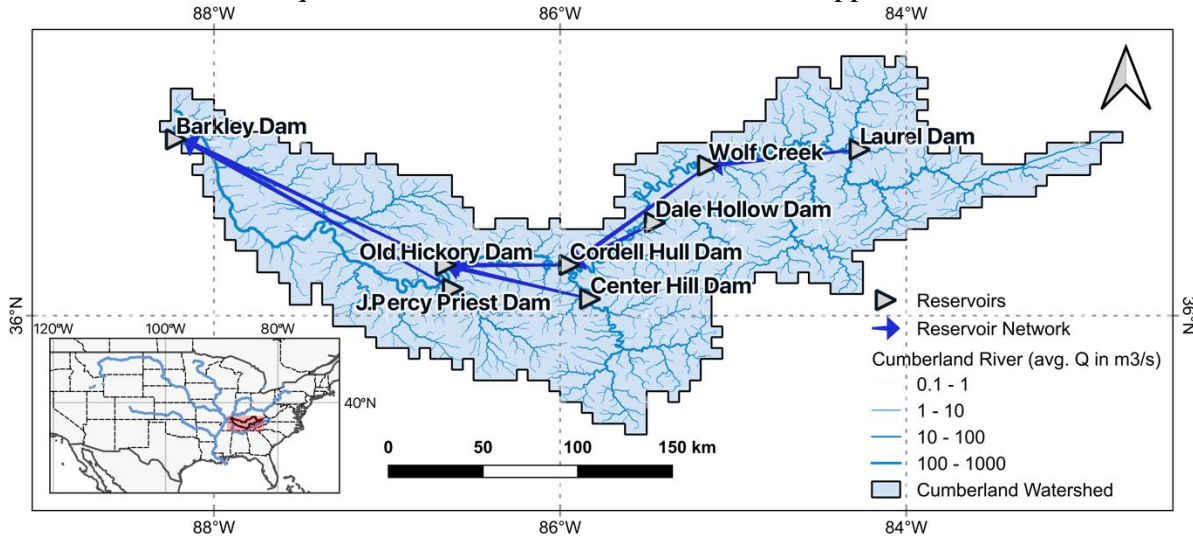


Figure 2 by traversing down the network of reservoirs for each time-step. To assess the performance of the model, sensitivity to uncertainties in the model inputs, and generally investigate the limitations of the model, various experiments were setup which are discussed in section 4.1.

To test the theoretical robustness of the proposed river regulation algorithm as a mass conserving scheme, we set up a two inter-connected linear reservoir problem where outflow is proportional to water storage and according to the elevation head available at the outlet. Using this set up we generated regulated inflow that should theoretically happen at the second reservoir

(reservoir 2) based on storage and regulation effect of the upstream reservoir (reservoir 1). Consequently, we tested the algorithm's ability to mimic the same regulated inflow to reservoir 2 using storage and upstream unregulated inflow of reservoir 1 that would be available in a globally scalable manner from satellite observations and modeling platforms such as RAT 3.0. Our algorithm demonstrated perfect theoretical consistency as a mass conserving scheme. More details on this theoretical robustness check of the algorithm are provided in the appendix (section 8).

3.2. Reservoir network

The reservoir network represents the connectivity of the reservoirs in the model and is represented by a directed tree data structure, with the nodes representing the reservoirs and the links depicting their connectivity, while preserving the order of reservoirs. The model first topologically sorts the reservoir network, to order them such that the water balance computations of upstream reservoirs are performed before the subsequent downstream reservoir. At each time-step, the model iterates over the topologically sorted reservoir network, and solves the series of equations discussed in 3.1.

The reservoir network is generated using the location of reservoirs and the Global Dominant River Tracing (DRT) dataset (Wu et al., 2011). Since the river-regulation model is designed as an add-on to the RAT framework, the script to generate the reservoir network can use the inputs and intermediary outputs of RAT to generate the reservoir network.





4. Experiments and Results

4.1. River regulation experiment setups using in-situ data

The ResORR algorithm is fully described by equations (1)-(5), which uses estimates of streamflow under pristine conditions from a hydrological model. However, the uncertainties in the estimations of hydrological model may propagate as uncertainty in the river-regulation model. Experiments were performed to isolate the performance of the core of the algorithm, its ability to partition the inflow between the natural and regulated components using in-situ observations in place of hydrological model and satellite estimates. By reducing uncertainties in certain parts of the algorithm, the performance of the individual components could be investigated, shedding light on the sensitivity of the algorithm components to the input data accuracy. Moreover, the observed in-situ ΔS was used in these experiments to gauge the baseline performance of ResORR using best available reservoir operations data, avoiding the higher uncertainties normally associated with satellite estimates of storage change.

To investigate the strengths and weaknesses of ResORR, especially in terms of scalability, the experiment designs were iteratively modified and updated in order from E1 to E4 over the period of 2015-2019. Details about the experiment designs and the rationale behind the experiments are summarized in Table 1.

349 Table 1: Summary of the experiments performed on the river regulation model along with the
350 corresponding symbols used in the performance comparison plot (Figure 4).

Exp.	In-situ data used	Description	Rationale
E1 	ΔS	In-situ ΔS was used in eqn. (5) to estimate O. VIC hydrologic model was not calibrated for estimating natural inflow.	Uncertainties in satellite estimates of ΔS are minimized in this experiment.
E2 	O	Observed O was used in eqn. (3) to estimate RR.	Uncertainties in otherwise estimated O, due to uncertainties in modeled I are minimized. The RR obtained as such would reflect the “theoretically” best estimate of incoming regulated streamflow.
E3 	I, ΔS	Observed I was used in eqn. (4) only at the most upstream dam, where $NR = TNR = I$. In-situ ΔS was used in (5) to estimate O.	For upstream-most reservoirs all the incoming streamflow would be due to natural runoff, hence, by using the observed I, the uncertainties due to modeled I are minimized. The RR in this case would reflect the “theoretical best estimate” of the downstream regulated streamflow.
E4 	ΔS	In-situ ΔS was used in eq (5) to estimate O. The VIC hydrological model, forced with satellite data, was calibrated at upstream most dams of Center Hill Dam, Dale Hollow Dam, and Laurel Dam.	The modeled inflow to the upstream most dams were calibrated using the observed inflow, essentially, minimizing the uncertainties at the upstream boundary of the reservoir network. This represents the ResORR in its globally scalable form under the scenario of perfect ΔS .

351 The regulated inflows obtained at the 4 dams, which have at least one upstream dam were
352 compared against the observed inflow at those same dams. The comparison statistics measuring
353 the performance of the river regulation model against observed inflow data are summarized in
354 Figure 4. To understand how the river regulation algorithm is performing under various input
355 scenarios and assumptions, one should compare the relative position of the symbols for each dam
356 along the horizontal axis only. The TNR, obtained from the VIC hydrological model are denoted
357 using grey and black circles, corresponding to the streamflow modeled using default parameter
358 values and calibrated parameters. Formulation of performance metrics are provided in Appendix
359 (section 8).

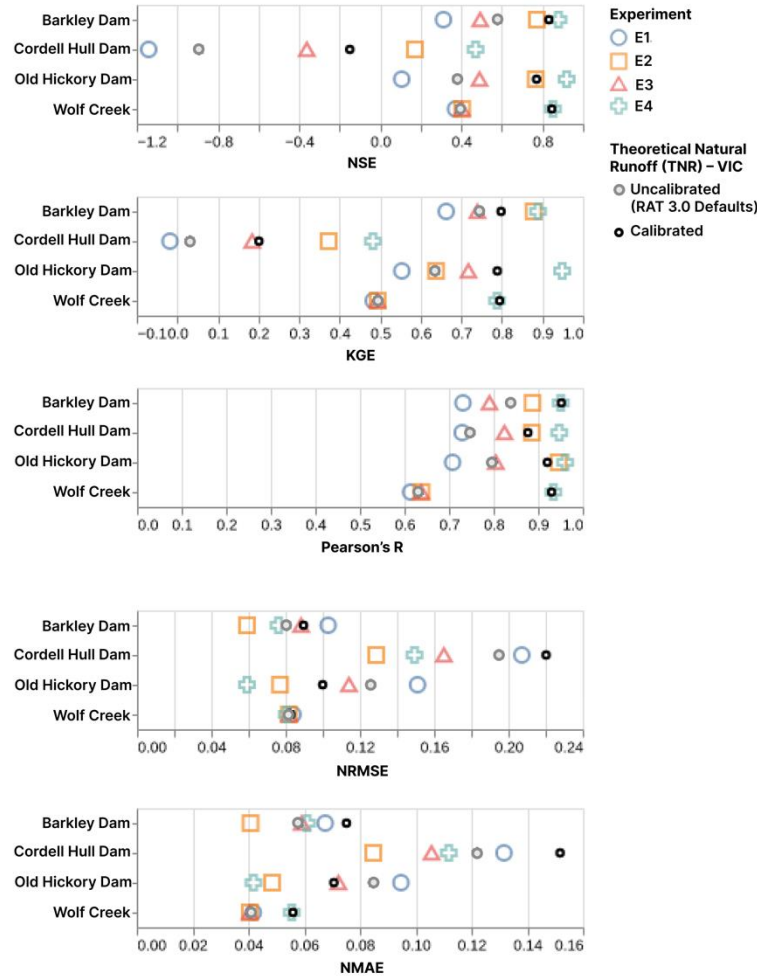


Figure 4: River regulation model performance for E* experiments using in-situ reservoir dynamics data.

Compared to the uncalibrated VIC streamflow estimates, the performance of the river regulation model in the E1 experiment in improving the accuracy of regulated inflow seems to be reduced. In other words, ResORR using in-situ ΔS , but with uncalibrated VIC flow at upstream most location does not improve the skill in predicted regulated inflow at downstream dam locations. However, on taking a closer look at the hydrographs comparing modeled inflow, TNR and observed inflow in Figure 5, it is apparent that the variability in the observed inflow, which is regulated inflow, is more closely replicated by the variability in the modeled inflow than the TNR. This likely suggests that even though the overall performance of ResORR gets reduced as a regulated streamflow predictor, the signature of human regulation is still captured well.

While analyzing the observed inflow hydrographs of two consecutive dams (Cordell Hull and Old Hickory dams) in Figure 6, a closer relationship between the downstream inflow and upstream outflow can be noted. It is clear that the upstream outflow plays a dominant role in dictating the downstream and regulated inflow at the next downstream dam as would be normally expected in the event of no lateral flow diversion. This relationship is further explored in the E2 experiment, where the daily in-situ outflow is used to calculate the RR to the downstream dam. Overall, the results improve across the board in the E2 experiment, underlining the role of upstream reservoir releases in predicting the downstream regulated streamflow. The

E2 experiment also stresses the importance of having high accuracy estimates of reservoir storage data.

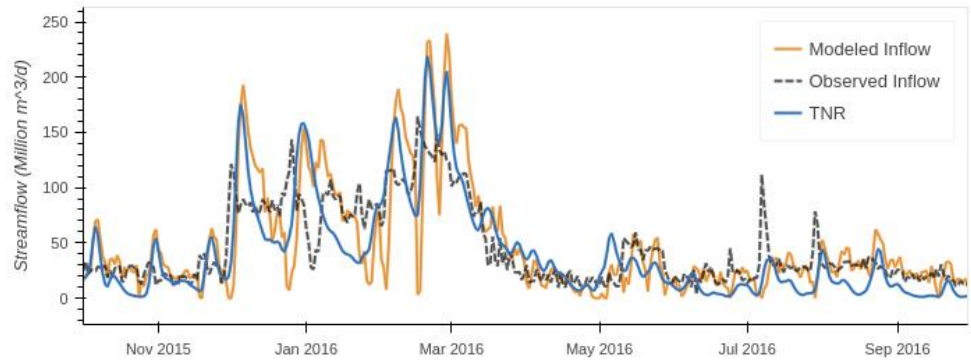


Figure 5: Hydrographs comparing the Modeled, Observed and TNR at Old Hickory Dam, which is the second most downstream dam in the network. The observed inflow is regulated inflow.

In the E3 experiment, the observed inflow to the upstream most dams was used as the NR. In most cases, the performance of the streamflow predictions still improved when adjusted for upstream regulation, as compared to the TNR. While this experiment suggests that if the accuracy of inflow estimates at the upstream most boundary conditions are accurate, that can improve the regulated streamflow estimates along that downstream network as well. Following this, the final E4 experiment, representative of the performance of the proposed and scalable river regulation model under accurate ΔS was performed. Here the VIC hydrological model was calibrated using the observed inflow at the upstream most dams. The result of this experiment shows the most significant improvement in the performance across all experiments. The performance of both the TNR, and the estimated regulated inflow improves in this case, nearly in all dams.

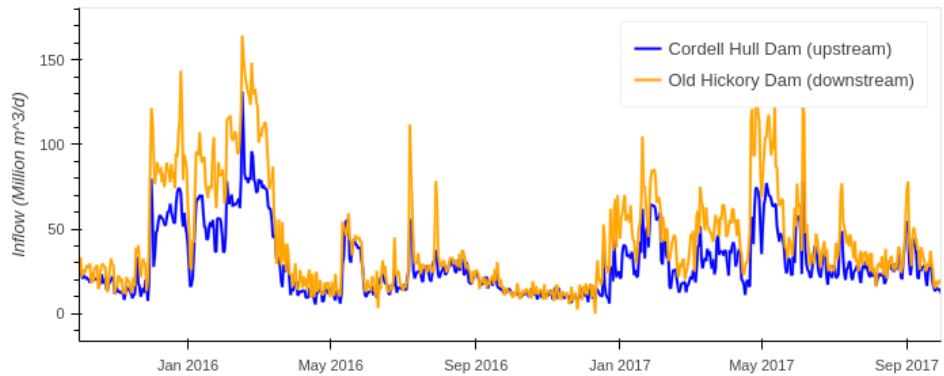


Figure 6: Observed inflows at two consecutive dams. The upstream Cordell Hull Dam drains into the downstream Old Hickory Dam, with the effect of upstream reservoir dynamics.

Moreover, the experiment results also shed light on the relationship between the model performance and the number of upstream dams. For instance, taking the case of the Wolf Creek dam (7.4 km^3 storage capacity), which only has one upstream dam (Laurel Dam, 0.5 km^3 storage capacity), the performance of the model does not improve as significantly as compared to the TNR. On the other hand, Cordell Hull Dam (run-of-the-river) is highly regulated and has two upstream dams, the Dale Hollow dam (2.1 km^3) and the Wolf Creek dam, and the performance of the streamflow estimates improves significantly by almost 50% across all the dams in the

basin. Overall, the results show that considering the effect of upstream regulation improves the performance of the streamflow estimates at the downstream dams.

4.2. River regulation using satellite estimates of reservoir storage change

Now that E4 results established robustness of the proposed river regulation algorithm, we explore how well ResORR fares with satellite-derived ΔS that will have higher uncertainty. The inundation area of the reservoirs were obtained using the Landsat-8 and Sentinel-1 satellite data from June 2018 to October 2021, using the TMS-OS algorithm described by Das et al., (2022). The storage change of the reservoirs were then obtained using these surface area estimates and in-situ Area-Elevation Curve (AEC), using the following equation –

$$\Delta S_t = \frac{A_t + A_{t-1}}{2} \times (h_t - h_{t-1}) \quad (6)$$

Here the ΔS in equation 6 is the total volumetric storage change, A is the inundation area, and h is the water level height corresponding to the inundation area, obtained using the AEC relationship. The date of satellite observation is denoted by t , with $t - 1$ referring to the last satellite observation. For instance, since Landsat-8 has a revisit period of 16 days, the estimated storage change would refer to the volumetric storage change within those 16 days. These storage change estimates were transformed to daily values by linearly distributing the volumetric change over 16 days. Based on the findings of the previous section, the VIC hydrological model was calibrated at the upstream most dams, like the E4 experiment. The modeled inflow as such and the streamflow estimates from VIC were compared against the observed in-situ inflow. The results are summarized in Figure 7.

Similar to the results in the previous section, for the Cordell Hull and Old Hickory, both run-of-the-river dams having upstream dams with large storage capacities, ResORR performance increases significantly across all metrics. For the Wolf Creek dam, adjusting for the upstream Laurel Dam's operations, ResORR performance does not increase as drastically, which can be explained due to the relatively smaller size of the upstream Laurel Dam. Unlike the in-situ data-based experiments, however, the model reduces the efficacy of inflow predictions for the Barkley dam as compared to the TNR. This can be explained by the run-of-the-river nature of the upstream dams, the storage change dynamics of which can be difficult to quantify using satellite observations. Overall, the results suggest that river regulation due to dams can be characterized by the proposed ResORR algorithm using satellite estimates of reservoir storage dynamics. Adjusting for flow regulation due to upstream reservoir storage change improves the overall inflow predictions in a regulated basin.

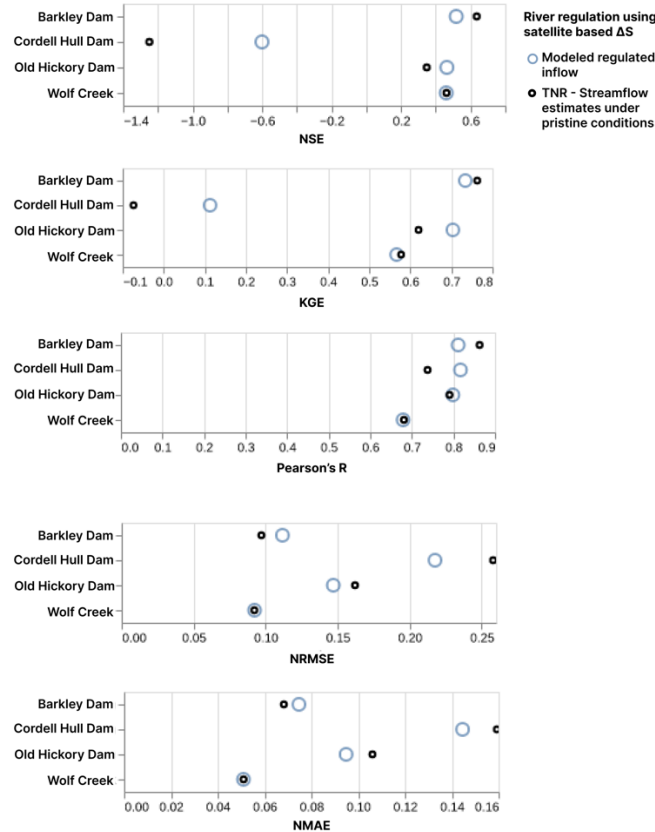


Figure 7: ResORR model performance using satellite derived reservoir storage change.

5. Scalability of ResORR - Case study of the 2018 floods in Kerala, India

In August 2018, the Indian state of Kerala experienced one of the worst cases of flooding in history due to an unexpectedly high precipitation event, which led to simultaneous release of water from 35 dams, leading to flooding at an unprecedented scale. The disaster claimed the lives of more than 480 people, displaced over 1.4 million and caused losses amounting to \$5.0 billion (Suresh et al., 2023). The main driving force of the disaster was the extremely high precipitation, when from June 1, 2018 to August 19, 2018, a span of only three months, the state received 42% more precipitation than expected. The situation was made even worse by the unpreparedness of the dams to absorb the high inflow of water due to a lack of sufficient flood cushioning, as all the dams were operating on a rigid rule curve optimized for hydropower generation. The flood primarily affected the Periyar River basin which impacted the districts of Ernakulam, Kollam, Alappuzha and Kottayam (figure 8).

Most dams in the basin serve a dual purpose of hydro-electric power generation and flood moderation, which is intrinsically conflicting in nature. The role played by the upstream dam releases during the flooding of the basin and the basin's unique topographical and climatic characteristics make it a perfect case study for testing the scalability of ResORR using only satellite observations of reservoir state.

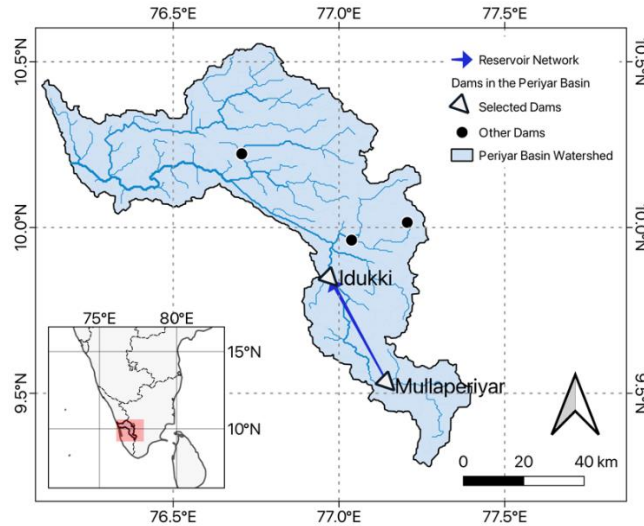


Figure 8: Map of the Periyar river basin showing the locations of Idukki and Mullaperiyar reservoirs and the reservoir network.

RAT 3.0 was setup over the Periyar basin to obtain satellite estimates of reservoir dynamics at a 1–5-day temporal frequency, including surface area and storage change estimates from April 2018 to October 2018 using the TMS-OS algorithm. The reservoir network and the TNR were obtained from the intermediary outputs of RAT 3.0. The VIC hydrological model used in the RAT setup was also calibrated manually. The model was then run using the satellite-observed reservoir dynamics and the modeled TNR. The hydrographs comparing the modeled regulated inflow to the Idukki dam are shown in Figure 9. For more details on the RAT 3.0 set up and the use of satellite observation for storage change estimation, readers are referred to Suresh et al. (2023).

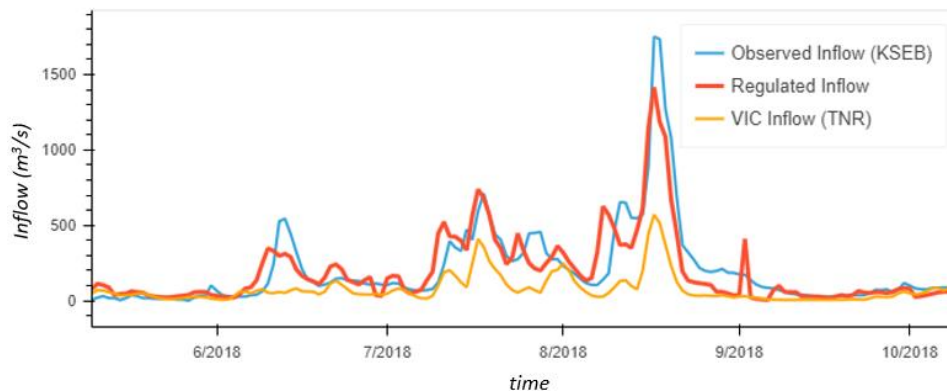


Figure 9: Hydrographs comparing modeled regulated inflow from ResORR (red) and TNR (orange as VIC inflow) against observed inflow (in blue as KSEB, which is regulated inflow) to the Idukki dam during the 2018 floods. In-situ reservoir inflow data at Idukki dam provided by Kerala State Electricity Board (KSEB).

Applying ResORR significantly improves the performance of the predicted inflow to the Idukki dam as compared to just using VIC, which models streamflow under unregulated conditions. The results also agree with the official reports, according to which large volumes of inflow was received from the Mullaperiyar dam, leading to a rapid deterioration of the storage capacity of Idukki, following which all 5 shutters of the dam were forced to be opened. The overall

prediction of downstream streamflow also improves drastically as evident from the comparison metrics summarized in

Table 2. The performance of the streamflow predictions improves across the board, especially the NSE and KGE metrics which improve significantly from 0.23 to 0.78 and 0.074 to 0.81, respectively. This demonstrates both, the important role played by the untimely release of water from the upstream Mullaperiyar dam during the 2018 floods, and the ability of the ResORR algorithm to correctly predict river regulation using only satellite observations.

Table 2: Statistics comparing the TNR and modeled inflow using ResORR against observed inflow at the Idukki dam for the August 2018 Kerala floods.

	<i>NSE</i>	<i>KGE</i>	<i>Pearson Correlation</i>	<i>Normalized RMSE</i>	<i>Normalized MAE</i>
<i>TNR</i>	0.233	0.074	0.833	0.137	0.077
<i>Modeled Regulated Inflow by ResORR</i>	0.78	0.81	0.884	0.074	0.047

6. Conclusions and Discussion

Rivers of the 21st century are marked with numerous reservoirs, which store, and release water based on their primary objectives, playing a vital role in providing food, water, and energy security. However, such reservoir operations can alter the natural streamflow patterns, reducing the water availability downstream by storing water during high flows, and *vice versa*. In this study, we developed and tested a scalable and globally applicable river regulation model, ResORR, to predict the regulation of streamflow due to upstream reservoir operations. Overall, we find that adjusting for upstream reservoir operations via storage change improves the accuracy of downstream streamflow predictions. The theoretical basis of the ResORR model was tested using in-situ data in the heavily regulated Cumberland basin. The results stress the importance of having high accuracy estimates of both the storage change and the hydrological model. Moreover, we find that if the hydrological model can be calibrated for boundary conditions of the reservoir network, *i.e.*, at the upstream most dams, significant improvement can be achieved in predicting regulated inflow at all the downstream dam locations.

We also tested the scalability of ResORR by applying it over a completely independent basin in Kerala, India. Using satellite observations alone, the model drastically improves the downstream streamflow predictions. The role played by upstream reservoir releases during the massive flood in 2018 that ravaged the entire state of Kerala was also captured by the model, significantly improving the prediction of the timing and intensity of the flood peak that ravaged the entire state of Kerala.

Currently, the reservoir network is automatically generated using the dam locations and the DRT flow directions, and hence, any inter- or intra-basin diversions between reservoirs or lateral diversions cannot yet be modeled. The regulation caused by reservoirs is also determined

by its storage capacity, and in a case where a small reservoir drains into a larger reservoir, the algorithm adds little value to the streamflow predictions. Even with these limitations, the ResORR algorithm can play an important role in quantifying the regulation of river flow due to reservoirs in changing the world's river systems.

With advancements in satellite observations-based reservoir dynamics tracking, especially the RAT 3.0, which has democratized access to reservoir operations information, it is now possible to easily track the operations of reservoirs globally. Building on top of the RAT framework, the proposed river regulation algorithm ResORR would also be able to characterize the regulation of river flow using only satellite-tracked reservoir states at the global scale. The ResORR software architecture is also designed to work seamlessly within the RAT framework, i.e., it can run entirely using the RAT model outputs and intermediary files. With this river regulation tool, the RAT framework will be able to not only infer reservoir dynamics, but also quantify the regulation of streamflow caused by the upstream reservoir operations at the global scale. We can expect ResORR to soon become a truly scalable algorithm based on the globally available reservoir storage change data of unprecedented accuracy from the Surface Water and Ocean Topography mission.

8. Open Research

Data Availability Statement

The Reservoir Assessment Tool (RAT) 3.0 (Minocha et al., 2023) was used to obtain satellite estimates of unregulated streamflow estimates using its default options of models and datasets (Bennett et al., 2020; Hamman et al., 2018, p. 5; Liang et al., 1994; Schaperow et al., 2021) for reservoirs in both Cumberland and Kerala regions. The RAT 3.0 software with all documentation and tutorials is available at <http://ratdocs.io> and <https://www.satellitedams.net>. The ResOpsUS (Steyaert et al., 2022) dataset was used to obtain in-situ reservoir operations for reservoirs in the Cumberland basin. The Dominant River Tracing (DRT) flow directions (Wu et al., 2012) were used to generate the reservoir network. In-situ Area-Elevation relationships were digitized from the Water Control Manual documents for reservoirs in the Cumberland basin from the Corps Water Management System (CWMS) Data Dissemination repository. In-situ inflow data for reservoirs in Kerala were digitized from reports on 2018 floods by the Kerala State Electricity Board (KSEB). Compiled input data for running the ResORR model are available at zenodo (10.5281/zenodo.10086338). The model code developed during this study is available on GitHub (<https://github.com/UW-SASWE/ResORR>) under the MIT license. Documentation on ResORR is available at - <https://resorr.readthedocs.io/en/latest/>

Acknowledgements: This study was supported by NASA Applied Science grants from the Water Resources Program (80NSSC22K0918) and the Capacity Building Program (80NSSC23K0184). All co-authors from the University of Washington, co-author Lee from University of Houston, and co-author Andreadis from University of Massachusetts were supported by both these programs.

555 **Author role:**
556 Research implementation: Pritam Das
557 Research design, data, and manuscript writing: Pritam Das and Faisal Hossain
558 Data, software and manuscript editing: Sanchit Minocha, George Darkwah and Sarath Suresh
559 Data and manuscript editing: Hyongki Lee and Konstantinos Andreadis
560 Research design and manuscript editing: Miguel Laverde-Barajas and Perry Oddo

7. References

- Ahmad, S. K., Hossain, F., Holtgrieve, G. W., Pavelsky, T., & Galelli, S. (2021). Predicting the Likely Thermal Impact of Current and Future Dams Around the World. *Earth's Future*, 9(10), e2020EF001916. <https://doi.org/10.1029/2020EF001916>
- Alcamo, J., Döll, P., Henrichs, T., Kaspar, F., Lehner, B., Rösch, T., & Siebert, S. (2003). Development and testing of the WaterGAP 2 global model of water use and availability. *Hydrological Sciences Journal*, 48(3), 317–337. <https://doi.org/10.1623/hysj.48.3.317.45290>
- Bennett, A., Hamman, J., & Nijssen, B. (2020). MetSim: A Python package for estimation and disaggregation of meteorological data. *Journal of Open Source Software*, 5(47), 2042. <https://doi.org/10.21105/joss.02042>
- Biancamaria, S., Lettenmaier, D. P., & Pavelsky, T. M. (2016). The SWOT Mission and Its Capabilities for Land Hydrology. *Surveys in Geophysics*, 37(2), 307–337. <https://doi.org/10.1007/s10712-015-9346-y>
- Biemans, H., Haddeland, I., Kabat, P., Ludwig, F., Hutjes, R. W. A., Heinke, J., von Bloh, W., & Gerten, D. (2011). Impact of reservoirs on river discharge and irrigation water supply during the 20th century. *Water Resources Research*, 47(3). <https://doi.org/10.1029/2009WR008929>
- Biswas, N. K., & Hossain, F. (2022). A Multidecadal Analysis of Reservoir Storage Change in Developing Regions. *Journal of Hydrometeorology*, 23(1), 71–85. <https://doi.org/10.1175/JHM-D-21-0053.1>
- Biswas, N. K., Hossain, F., Bonnema, M., Lee, H., & Chishtie, F. (2021). Towards a global Reservoir Assessment Tool for predicting hydrologic impacts and operating patterns of

584 existing and planned reservoirs. *Environmental Modelling & Software*, 140, 105043.
585 <https://doi.org/10.1016/j.envsoft.2021.105043>

586 Bonnema, M., & Hossain, F. (2017). Inferring reservoir operating patterns across the Mekong
587 Basin using only space observations. *Water Resources Research*, 53(5), 3791–3810.
588 <https://doi.org/10.1002/2016WR019978>

589 Bonnet, M., Witt, A., Steart, K., Hadjerioua, B., & Mobley, M. (2015). *The Economic Benefits of*
590 *Multipurpose Reservoirs in the United States-Federal Hydropower Fleet*.
591 <https://doi.org/10.13140/RG.2.2.15894.14400>

592 Caissie, D. (2006). The thermal regime of rivers: A review. *Freshwater Biology*, 51(8), 1389–
593 1406. <https://doi.org/10.1111/j.1365-2427.2006.01597.x>

594 Cheng, Y., Nijssen, B., Holtgrieve, G. W., & Olden, J. D. (2022). Modeling the freshwater
595 ecological response to changes in flow and thermal regimes influenced by reservoir
596 dynamics. *Journal of Hydrology*, 608, 127591.
597 <https://doi.org/10.1016/j.jhydrol.2022.127591>

598 Cheng, Y., Voisin, N., Yearsley, J. R., & Nijssen, B. (2020). Reservoirs Modify River Thermal
599 Regime Sensitivity to Climate Change: A Case Study in the Southeastern United States.
600 *Water Resources Research*, 56(6), e2019WR025784.
601 <https://doi.org/10.1029/2019WR025784>

602 Cooley, S. W., Ryan, J. C., & Smith, L. C. (2021). Human alteration of global surface water
603 storage variability. *Nature*, 591(7848), Article 7848. [https://doi.org/10.1038/s41586-021-](https://doi.org/10.1038/s41586-021-03262-3)
604 [03262-3](https://doi.org/10.1038/s41586-021-03262-3)

605 Das, P., Hossain, F., Khan, S., Biswas, N. K., Lee, H., Piman, T., Meechaiya, C., Ghimire, U., &
606 Hosen, K. (2022). Reservoir Assessment Tool 2.0: Stakeholder driven improvements to

satellite remote sensing based reservoir monitoring. *Environmental Modelling & Software*, 157(105533). <https://doi.org/10.1016/j.envsoft.2022.105533>

Dunn, F. E., Darby, S. E., Nicholls, R. J., Cohen, S., Zarfl, C., & Fekete, B. M. (2019). Projections of declining fluvial sediment delivery to major deltas worldwide in response to climate change and anthropogenic stress. *Environmental Research Letters*, 14(8), 084034. <https://doi.org/10.1088/1748-9326/ab304e>

Earth Resources Observation And Science (EROS) Center. (2017). *Shuttle Radar Topography Mission (SRTM) 1 Arc-Second Global* [Tiff]. U.S. Geological Survey. <https://doi.org/10.5066/F7PR7TFT>

Eldardiry, H., & Hossain, F. (2021). A blueprint for adapting high Aswan dam operation in Egypt to challenges of filling and operation of the Grand Ethiopian Renaissance dam. *Journal of Hydrology*, 598, 125708. <https://doi.org/10.1016/j.jhydrol.2020.125708>

Gao, H., Birkett, C., & Lettenmaier, D. P. (2012). Global monitoring of large reservoir storage from satellite remote sensing. *Water Resources Research*, 48(9), 2012WR012063. <https://doi.org/10.1029/2012WR012063>

Gupta, H. V., Kling, H., Yilmaz, K. K., & Martinez, G. F. (2009). Decomposition of the mean squared error and NSE performance criteria: Implications for improving hydrological modelling. *Journal of Hydrology*, 377(1–2), 80–91. <https://doi.org/10.1016/j.jhydrol.2009.08.003>

Haddeland, I., Skaugen, T., & Lettenmaier, D. P. (2006). Anthropogenic impacts on continental surface water fluxes. *Geophysical Research Letters*, 33(8), L08406. <https://doi.org/10.1029/2006GL026047>

629 Hamman, J. J., Nijssen, B., Bohn, T. J., Gergel, D. R., & Mao, Y. (2018). The Variable
630 Infiltration Capacity model version 5 (VIC-5): Infrastructure improvements for new
631 applications and reproducibility. *Geoscientific Model Development*, 11(8), 3481–3496.
632 <https://doi.org/10.5194/gmd-11-3481-2018>Hanasaki, N., Kanae, S., & Oki, T. (2006). A
633 reservoir operation scheme for global river routing models. *Journal of Hydrology*, 327(1–
634 2), 22–41. <https://doi.org/10.1016/j.jhydrol.2005.11.011>

635 Hanasaki, N., Yoshikawa, S., Pokhrel, Y., & Kanae, S. (2018). A global hydrological simulation
636 to specify the sources of water used by humans. *Hydrology and Earth System Sciences*,
637 22(1), 789–817. <https://doi.org/10.5194/hess-22-789-2018>

638 Hersbach, H., Bell, B., Berrisford, P., Hirahara, S., Horányi, A., Muñoz-Sabater, J., Nicolas, J.,
639 Peubey, C., Radu, R., Schepers, D., Simmons, A., Soci, C., Abdalla, S., Abellan, X.,
640 Balsamo, G., Bechtold, P., Biavati, G., Bidlot, J., Bonavita, M., ... Thépaut, J. (2020).
641 The ERA5 global reanalysis. *Quarterly Journal of the Royal Meteorological Society*,
642 146(730), 1999–2049. <https://doi.org/10.1002/qj.3803>

643 Hossain, F., Sikder, S., Biswas, N., Bonnema, M., Lee, H., Luong, N. D., Hiep, N. H., Du
644 Duong, B., & Long, D. (2017). Predicting Water Availability of the Regulated Mekong
645 River Basin Using Satellite Observations and a Physical Model. *Asian Journal of Water,*
646 *Environment and Pollution*, 14(3), 39–48. <https://doi.org/10.3233/AJW-170024>

647 Knoben, W. J. M., Freer, J. E., & Woods, R. A. (2019). *Technical note: Inherent benchmark or*
648 *not? Comparing Nash-Sutcliffe and Kling-Gupta efficiency scores* [Preprint]. Catchment
649 hydrology/Modelling approaches. <https://doi.org/10.5194/hess-2019-327>

650 Lee, H., Durand, M., Jung, H. C., Alsdorf, D., Shum, C. K., & Sheng, Y. (2010).
651 Characterization of surface water storage changes in Arctic lakes using simulated SWOT

652 measurements. *International Journal of Remote Sensing*, 31(14), 3931–3953.
653 <https://doi.org/10.1080/01431161.2010.483494>

654 Li, S., Xu, Y. J., & Ni, M. (2021). Changes in sediment, nutrients and major ions in the world
655 largest reservoir: Effects of damming and reservoir operation. *Journal of Cleaner*
656 *Production*, 318, 128601. <https://doi.org/10.1016/j.jclepro.2021.128601>

657 Liang, X., Lettenmaier, D. P., Wood, E. F., & Burges, S. J. (1994). A simple hydrologically
658 based model of land surface water and energy fluxes for general circulation models.
659 *Journal of Geophysical Research: Atmospheres*, 99(D7), 14415–14428.
660 <https://doi.org/10.1029/94JD00483>

661 Marcaida, M., Farhat, Y., Muth, E.-N., Cheythyrih, C., Hok, L., Holtgrieve, G., Hossain, F.,
662 Neumann, R., & Kim, S.-H. (2021). A spatio-temporal analysis of rice production in
663 Tonle Sap floodplains in response to changing hydrology and climate. *Agricultural Water*
664 *Management*, 258, 107183. <https://doi.org/10.1016/j.agwat.2021.107183>

665 Minocha, S., Hossain, F., Das, P., Suresh, S., Khan, S., Darkwah, G., Lee, H., Galelli, S.,
666 Andreadis, K., & Oddo, P. (2023). *Reservoir Assessment Tool Version 3.0: A Scalable*
667 *and User-Friendly Software Platform to Mobilize the Global Water Management*
668 *Community* [Preprint]. Hydrology. <https://doi.org/10.5194/gmd-2023-130>

669 Nash, J. E., & Sutcliffe, J. V. (1970). River flow forecasting through conceptual models part I —
670 A discussion of principles. *Journal of Hydrology*, 10(3), 282–290.
671 [https://doi.org/10.1016/0022-1694\(70\)90255-6](https://doi.org/10.1016/0022-1694(70)90255-6)

672 Neel, J. K., & Allen, W. R. (1964). The mussel fauna of the upper Cumberland Basin before its
673 impoundment. *Malacologia*, 1(3), 427–459.

674 Okeowo, M. A., Lee, H., Hossain, F., & Getirana, A. (2017). Automated Generation of Lakes
 675 and Reservoirs Water Elevation Changes From Satellite Radar Altimetry. *IEEE Journal*
 676 *of Selected Topics in Applied Earth Observations and Remote Sensing*, 10(8), 3465–
 677 3481. <https://doi.org/10.1109/JSTARS.2017.2684081>

678 Pokhrel, Y., Shin, S., Lin, Z., Yamazaki, D., & Qi, J. (2018). Potential Disruption of Flood
 679 Dynamics in the Lower Mekong River Basin Due to Upstream Flow Regulation.
 680 *Scientific Reports*, 8(1), Article 1. <https://doi.org/10.1038/s41598-018-35823-4>

681 Robinson, J. A. (2019). *Estimated use of water in the Cumberland River watershed in 2010 and*
 682 *projections of public-supply water use to 2040* (Report 2018–5130; Scientific
 683 Investigations Report, p. 74). USGS Publications Warehouse.
 684 <https://doi.org/10.3133/sir20185130>

685 Schaperow, J. R., Li, D., Margulis, S. A., & Lettenmaier, D. P. (2021). A near-global, high
 686 resolution land surface parameter dataset for the variable infiltration capacity model.
 687 *Scientific Data*, 8(1), 216. <https://doi.org/10.1038/s41597-021-00999-4>

688 Steyaert, J. C., Condon, L. E., W. D. Turner, S., & Voisin, N. (2022). ResOpsUS, a dataset of
 689 historical reservoir operations in the contiguous United States. *Scientific Data*, 9(1),
 690 Article 1. <https://doi.org/10.1038/s41597-022-01134-7>

691 Suresh, S., Hossain, F., Minocha, S., Das, P., Khan, S., Lee, H., Andreadis, K., & Oddo, P.
 692 (2023). Satellite-based Tracking of Reservoir Operations for Flood Management during
 693 the 2018 Extreme Weather Event in Kerala, India. *Remote Sensing of the Environment*
 694 *(In review)* Available online at <https://saswe.net/publications/RATKerala.pdf>

695 Tippit, R. N., Brown, J. K., Sharber, J. F., & Miller, A. C. (1995). Modifying Cumberland River
 696 system reservoir operations to improve mussel habitat. *Conservation and Management of*

697 *Freshwater Mussels II: Initiatives for the Future. Proceedings of a UMRCC Symposium,*
698 229–235.

699 USACE. (n.d.). *WM Data Dissemination*. Retrieved October 15, 2023, from
700

701 Vanderkelen, I., Gharari, S., Mizukami, N., Clark, M. P., Lawrence, D. M., Swenson, S.,
702 Pokhrel, Y., Hanasaki, N., van Griensven, A., & Thiery, W. (2022). Evaluating a
703 reservoir parametrization in the vector-based global routing model mizuRoute (v2.0.1)
704 for Earth system model coupling. *Geoscientific Model Development*, 15(10), 4163–4192.
705 <https://doi.org/10.5194/gmd-15-4163-2022>

706 Vu, D. T., Dang, T. D., Galelli, S., & Hossain, F. (2021). Satellite observations reveal thirteen
707 years of reservoir filling strategies, operating rules, and hydrological alterations in the
708 Upper Mekong River Basin [Preprint]. *Hydrology Earth System Science*.
709 <https://doi.org/10.1002/essoar.10507302.1>

710 Wada, Y., Bierkens, M. F. P., de Roo, A., Dirmeyer, P. A., Famiglietti, J. S., Hanasaki, N.,
711 Konar, M., Liu, J., Müller Schmied, H., Oki, T., Pokhrel, Y., Sivapalan, M., Troy, T. J.,
712 van Dijk, A. I. J. M., van Emmerik, T., Van Huijgevoort, M. H. J., Van Lanen, H. A. J.,
713 Vörösmarty, C. J., Wanders, N., & Wheeler, H. (2017). Human–water interface in
714 hydrological modelling: Current status and future directions. *Hydrology and Earth*
715 *System Sciences*, 21(8), 4169–4193. <https://doi.org/10.5194/hess-21-4169-2017>

716 Wilson, C. B., & Clark, H. W. (1914). *The mussels of the Cumberland River and its tributaries*
717 (Issue 781). US Government Printing Office.

718 Wissler, D., & Fekete, B. M. (2009). *Reconstructing 20th century global hydrography*.

719 Wu, H., Kimball, J. S., Mantua, N., & Stanford, J. (2011). Automated upscaling of river
720 networks for macroscale hydrological modeling: Upscaling f Global River Networks.
721 *Water Resources Research*, 47(3).

722 Wu, H., Kimball, J. S., Li, H., Huang, M., Leung, L. R., & Adler, R. F. (2012). A new global
723 river network database for macroscale hydrologic modeling. *Water Resources Research*,
724 48(9), 2012WR012313.
725 <https://doi.org/10.1029/2012WR012313><https://doi.org/10.1029/2009WR008871>

726 Zhao, G., Li, Y., Zhou, L., & Gao, H. (2022). Evaporative water loss of 1.42 million global
727 lakes. *Nature Communications*, 13(1), 3686. <https://doi.org/10.1038/s41467-022-31125-6>

728 Zhou, T., Nijssen, B., Gao, H., & Lettenmaier, D. P. (2016). The Contribution of Reservoirs to
729 Global Land Surface Water Storage Variations. *Journal of Hydrometeorology*, 17(1),
730 309–325. <https://doi.org/10.1175/JHM-D-15-0002.1>

731
732

8. Appendix

8.1. River-regulation in a theoretical two-reservoir system using synthetic data

A theoretical two inter-connected linear reservoir system with artificially generated headwater flow inputs was used to test the theoretical robustness of the mass conserving and numerical stability of the ResORR algorithm. This classic problem (Figure 10) also helped visualize the outputs of ResORR algorithm and verify if mass balance is maintained.

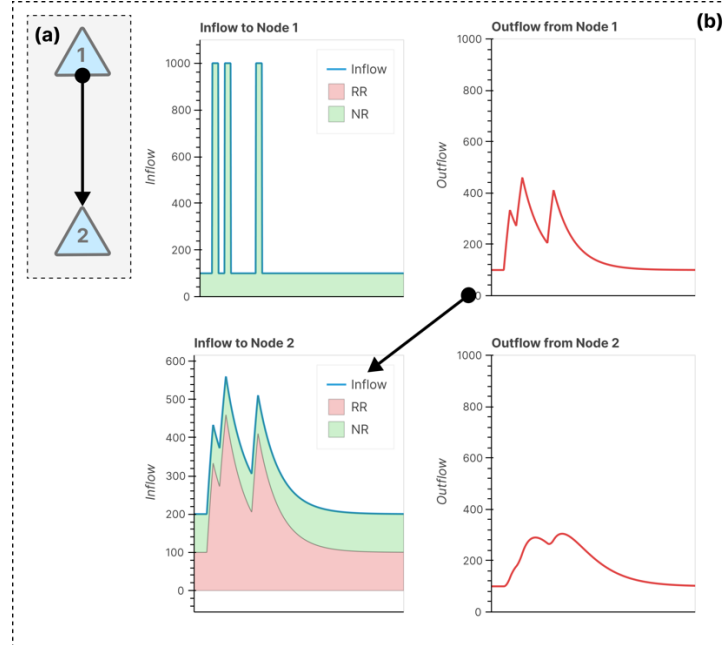


Figure 10: (a) Schematic showing the two-reservoir system setup. The black arrow denotes the direction of flow of water. (b) Hydrographs showing inflow and outflow from nodes 1 and 2. In this case, three input pulses of $1000 \text{ L}^3/\text{T}$ units were fed into node 1, and its outflow was treated as the inflow to the downstream node 2. The inflow and outflow at node 2 represent the ‘theoretical’ answer for the ResORR algorithm to be theoretically valid.

A system of two interconnected linear reservoirs were set up, like the schematic shown in Figure 10. To understand how the outflow from an upstream reservoir would affect the inflow to the downstream reservoir, we first generated a synthetic headwater inflow hydrograph for reservoir 1 and then applied ResORR to predict the regulated inflow to the downstream reservoir at node 2. Both the reservoirs were provided with a constant water influx of $100 \text{ L}^3/\text{T}$ units in the form of natural runoff, NR. Additionally, the upstream reservoir, at node 1, was provided with three pulses of high inflow volumes of $1000 \text{ L}^3/\text{T}$ units. The reservoirs were treated as linear reservoirs, where the outflow from a reservoir at any given time as a linear function of the instantaneous storage, and can be defined as follows –

$$O = K \times S$$

Where, $K [T^{-1}]$ is the reaction factor, which determines how quickly the reservoir drains ($K = 0.01$ in this experiment). The outflow from the upstream reservoir at node 1 was then treated as the regulated runoff, RR for the downstream reservoir, node 2. Using the inflows and

outflows obtained at both the reservoirs, the storage change was obtained using (5). The theoretical natural runoff, TNR, was also obtained using (3). The ResORR was then run using this simulated storage change and TNR information as inputs, to model the inflow at both the reservoirs. The modeled inflow of ResORR was then compared with the synthetically generated inflow at the downstream node 2, with a perfect match between them. The closure of water balance was also tested by comparing the total inflow volumes in the modeled and synthetic inflow.

8.2. Performance metrics used for assessing ResORR

The following five commonly used performance metrics were used in this study to quantify the skill of the river regulation model -

Metric	Equation	Description
Nash-Sutcliffe Efficiency (NSE) (Nash & Sutcliffe, 1970)	$1 - \frac{\sum_{t=1}^T (Q_O^t - Q_M^t)^2}{\sum_{t=1}^T (Q_O^t - \bar{Q}_O)^2}$ <p>Where, Q_O^t and Q_M^t are observed and modeled streamflow respectively. \bar{Q}_O is the mean observed streamflow.</p>	The NSE can vary between $-\infty$ and 1. A value of 1 indicates a perfect match between observed and modeled values. A value of 0 indicates that the model predictions are as performant as using the mean of the observed values as a predictor. Higher values are better.
Kling-Gupta Efficiency (KGE) (Gupta et al., 2009)	$1 - \sqrt{(r - 1)^2 + (\alpha - 1)^2 + (\beta - 1)^2}$ <p>Where, r is the linear correlation between modeled and observed values, $\alpha = \left(\frac{\sigma_M}{\sigma_O} - 1\right)^2$, σ_M and σ_O are the standard deviations of the modeled and observed values, $\beta = \left(\frac{\mu_M}{\mu_O} - 1\right)^2$, μ_M and μ_O are mean modeled and observed values.</p>	The KGE varies between $-\infty$ and 1. A value of -0.41 indicates model performance equal to using the mean of the observed values as a predictor (Knoben et al., 2019). Higher values are better.
Pearson's R	$\frac{cov(Q_O, Q_M)}{\sigma_O \sigma_M}$ <p>Where, $cov(Q_O, Q_M)$ is the covariance of the observed and modeled values. σ_M and σ_O are the standard deviations of the modeled and observed values</p>	The Pearson's R can vary from -1 to 1, where 1 indicates a perfect positive linear correlation. A value of 0 indicates no correlation.
Normalized Root-Mean Squared Error (NRMSE)	$\frac{\sqrt{\frac{\sum_{i=1}^N (Q_O - Q_M)^2}{N}}}{\max(Q_O) - \min(Q_O)}$ <p>Where, $\max(Q_O)$ and $\min(Q_O)$ are the maximum and minimum observed</p>	The NRMSE represents the standard deviation of the residuals as a fraction of the range of the observed values. Lower values are better.

	streamflow values.	
Normalized Mean Absolute Error (NMAE)	$\frac{\sum_{i=1}^N Q_M - Q_O }{N \cdot \max(Q_O) - \min(Q_O)}$ <p>Where, N is the number of observations, $Q_M - Q_O$ is the absolute difference of modeled and observed values</p>	The NMAE represents the average absolute difference between observed and modeled values as a fraction of the range of observed values. Lower values are better.

8.3. Handling missing In-situ storage data

Two dams in the basin, Old Hickory and Laurel, had missing in-situ storage data after April 2015, due to which storage change could not be calculated using observed (in-situ) storage. This missing data was filled by assuming water mass-balance owing to inflow and outflow from the reservoirs, $\Delta S = I - O$.

